**Zeitschrift:** IABSE reports of the working commissions = Rapports des commissions de travail AIPC = IVBH Berichte der Arbeitskommissionen

**Band:** 11 (1971)

**Artikel:** Ultimate strength of plates when subjected to in-plane patch loading

**Autor:** Rockey, K.C. / El-Gaaly, M.A.

**DOI:** https://doi.org/10.5169/seals-12076

III

# Ultimate Strength of Plates When Subjected to In-Plane Patch Loading

Résistance à la ruine des âmes soumises à des charges transversales locales

Tragfähigkeit von Stehblechfeldern bei örtlicher Randstreckenlast

**K.C. ROCKEY**
M.Sc., Ph.D., C.Eng., F.I.C.E.
Professor of Civil
and Structural Engineering

**M.A. EL-GAALY**
M.S.E., D.Sc., M.ASCE.
Research Fellow
Department of Civil
and Structural Engineering

University College, Cardiff, England

## 1. INTRODUCTION

Frequently web plates are subjected to local in-plane compressive patch loading, such as that shown in figure 1. If the depth to thickness ratio of the web is sufficiently high then it will buckle before it fails. Such web buckling is not synonymous with failure but simply represents a transition from one load carrying mechanism to another load carrying mechanism and the present study has been conducted to obtain relationships between the ultimate load capacity of a panel and its buckling load.

The test program involved a study of how the ultimate load varied with the loading parameter $\beta$ (= c/b), the panel aspect ratio $\alpha$ (= b/d) and the slenderness ratio (d/t). It will be shown that a linear relationship exists between the ratio of the ultimate load to the buckling load of a panel and its slenderness ratio $\frac{d}{t}$ and the loading parameter, $\beta$.

## 2. ELASTIC BUCKLING LOADS

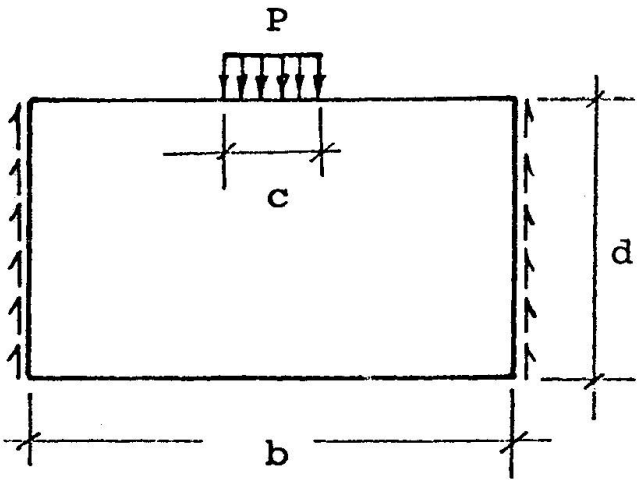


Fig. 1

Theoretical critical load values have been determined for the buckling of plates when subjected to uniform edge load and also for the more difficult case of a panel subjected to partial edge loading (1 - 10). Rockey and Bagchi (10) used the Finite Element Method to determine the buckling load of a rectangular panel when subjected to a patch load on one longitudinal edge and supported by shear forces on the two transverse edges as shown in figure 1. Results were also obtained for the cases where an in-plane moment or an in-plane

shear stress acts in addition to the stress field set up by the patch loading.

The compressive patch load ($P_{cr}$) which will cause buckling of a rectangular plate is given by equation (1).

$$\frac{P_{cr}}{bt} = K \frac{\pi^2 D}{d^2 t} \qquad (1)$$

Figure 2, gives the relationship between the non-dimensional buckling coefficient K, the loading parameter $\beta$ (= c/b) and the aspect ratio $\alpha$ (= b/d).

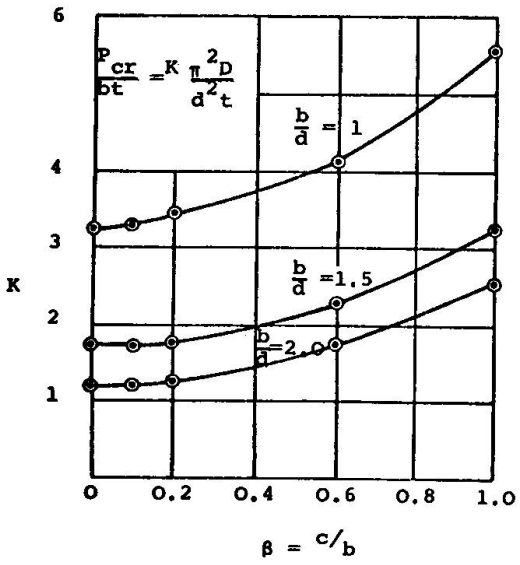


Fig. 2. Variation of the buckling coefficient K with the loading parameter $\beta$ and the panel aspect ratio b/d.

The presence of either an additional shear or moment will reduce the applied edge load necessary to buckle the panel. Figure 3 presents the interaction curves which have been obtained for the following two cases,

(i) a simply supported square plate subject to a combination of uniform edge-loading and in-plane moment

(ii) a simply supported square plate subject to a combination of discrete edge loading ($\beta$ = 0.2) and in-plane moment

Figure 4 gives the corresponding interaction curves for the combination of a transverse edge loading and an additional uniform shear load.

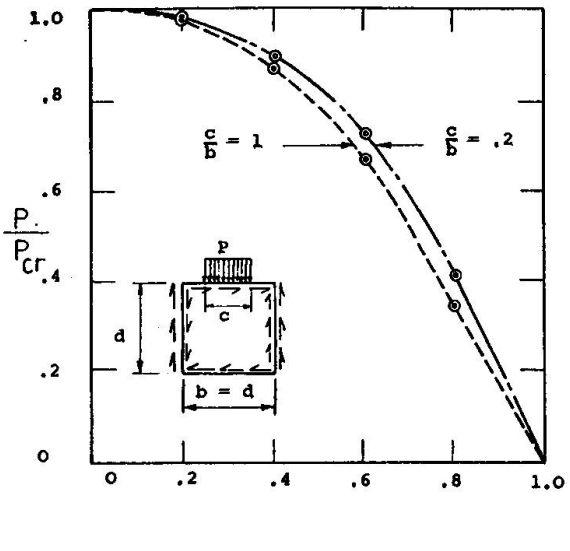


Fig. 3. Influence of a co-existent shear upon the magnitude of the critical patch load.

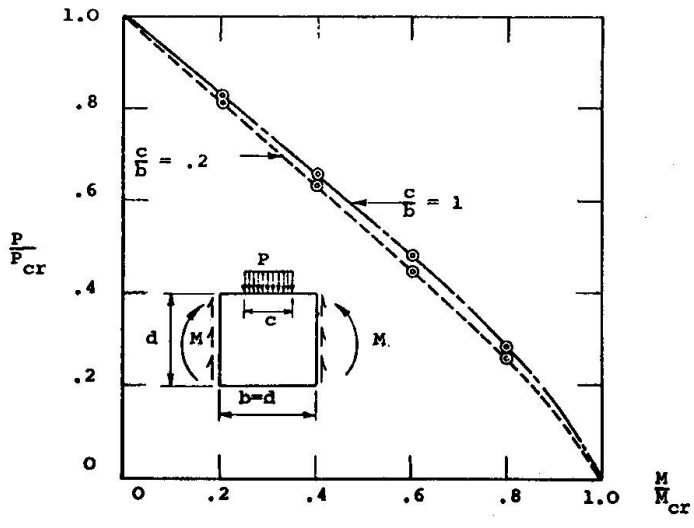


Fig. 4. Influence of a co-existent bending moment upon the magnitude of the critical patch load P.

## 3. TEST PROGRAM

The tests were conducted to determine the ultimate load strength characteristics of the webs of a sheet steel flooring system. Figure 5 shows the cross section of the unit (one bay) which was tested.

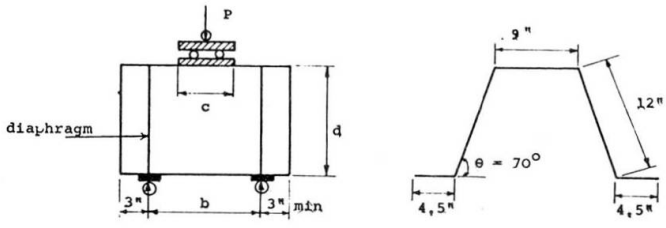


Fig. 5. Details of Test Specimen.

The test specimen was supported on roller supports which could be adjusted to ensure that the load was applied to both webs. At each support a very strong diaphragm was fitted and straps were fitted across the base of the specimen thus ensuring that no splaying of the webs would occur.

The specimens were tested in a self straining frame and the load was applied by means of a push type hydraulic ram through a central roller and was distributed over a distance c, as shown in figure 6. An electric load cell was placed between the ram and the test specimen as can be noted in the figure.

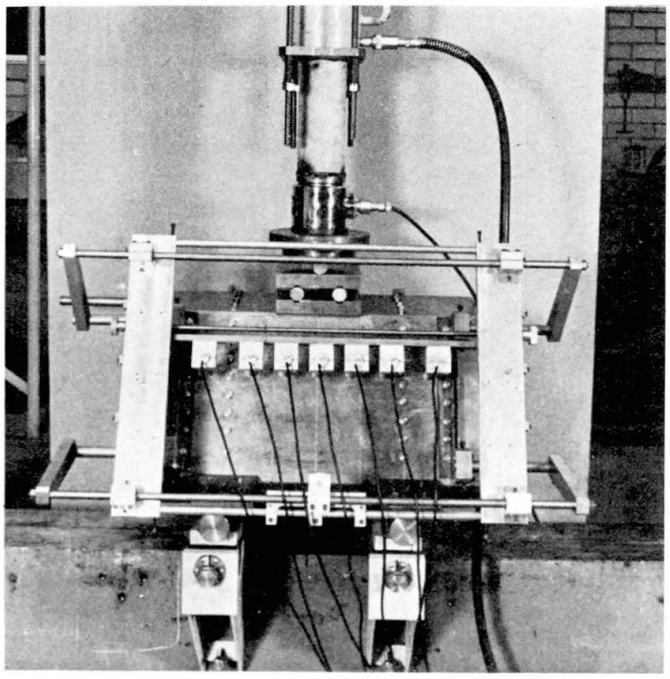

Fig. 6.

The lateral deflection of the web was recorded using the special deflection recording apparatus shown in figure 6. With the aid of this frame, the seven linear displacement transducers could be adjusted to any position. These transducers were connected to a data logger which printed out directly the values of the deflections in units of 0.001 inch. In addition, dial gauges, calibrated in units of 0.001 inch were used to record the lateral deflections at specific positions.

Loads were applied to the test specimens in small increments in the elastic range, and in smaller increments after yielding had begun. In the inelastic range, all plastic flow was allowed to take place at each load increment before any lateral deflection readings were taken.

To determine the material properties three test coupons were tested from each plate to determine the yield stresses and other material properties. All of the test coupons behaved in a manner typical of that expected for mild structural steel and the results showed that the yield stress did not vary markedly from one gauge of material to another.

## 4. EXPERIMENTAL RESULTS

TABLE 1.

| Test No. | d inch | b inch | c inch | t inch | $\alpha=\frac{b}{d}$ | $\beta=\frac{c}{b}$ | $\frac{d}{t}$ | $P_u$ tons | $P_{cr}$ tons | $\frac{P_u}{P_{cr}}$ |
|---|---|---|---|---|---|---|---|---|---|---|
| 1.1 | 12 | 12 | 2.4 | .037 | 1 | .2 | 325 | .37 | .17 | 2.17 |
| 1.2 | 12 | 12 | 2.4 | .048 | 1 | .2 | 250 | .54 | .38 | 1.43 |
| 1.3 | 12 | 12 | 2.4 | .06 | 1 | .2 | 200 | .84 | .74 | 1.13 |
| 1.4 | 12 | 12 | 2.4 | .075 | 1 | .2 | 160 | 1.30 | 1.43 | .91 |
| 1.5 | 12 | 12 | 2.4 | .102 | 1 | .2 | 118 | 2.56 | 3.58 | .72 |
| 1.6 | 12 | 12 | 2.4 | .128 | 1 | .2 | 94 | 4.20 | 7.08 | .59 |
| 2.1 | 12 | 12 | 6 | .037 | 1 | .5 | 325 | .58 | .19 | 3.06 |
| 2.2 | 12 | 12 | 6 | .048 | 1 | .5 | 250 | .85 | .43 | 1.98 |
| 2.3 | 12 | 12 | 6 | .06 | 1 | .5 | 200 | 1.23 | .83 | 1.48 |
| 2.4 | 12 | 12 | 6 | .075 | 1 | .5 | 160 | 2.04 | 1.61 | 1.27 |
| 2.5 | 12 | 12 | 6 | .102 | 1 | .5 | 118 | 3.95 | 4.04 | .98 |
| 2.6 | 12 | 12 | 6 | .128 | 1 | .5 | 94 | 6.08 | 7.96 | .76 |
| 3.1 | 12 | 12 | 1.2 | .06 | 1 | .1 | 200 | .71 | .70 | 1.01 |
| 3.2 | 12 | 12 | 2.4 | .06 | 1 | .2 | 200 | .84 | .74 | 1.13 |
| 3.3 | 12 | 12 | 3.6 | .06 | 1 | .3 | 200 | .97 | .76 | 1.27 |
| 3.4 | 12 | 12 | 4.8 | .06 | 1 | .4 | 200 | 1.1 | .80 | 1.38 |
| 3.5 | 12 | 12 | 6 | .06 | 1 | .5 | 200 | 1.23 | .83 | 1.48 |
| 4.1 | 12 | 18 | 3.6 | .037 | 1.5 | .2 | 325 | .41 | .13 | 3.15 |
| 4.2 | 12 | 18 | 3.6 | .048 | 1.5 | .2 | 250 | .54 | .29 | 1.90 |
| 4.3 | 12 | 18 | 3.6 | .06 | 1.5 | .2 | 200 | .86 | .57 | 1.51 |
| 4.4 | 12 | 18 | 3.6 | .102 | 1.5 | .2 | 118 | 2.5 | 2.77 | .90 |
| 4.5 | 12 | 18 | 3.6 | .128 | 1.5 | .2 | 94 | 4.10 | 5.49 | .75 |

The details of the test program are summarized in Table 1. In all the tests, the section was subjected to a patch load together with the reactive shear forces.

Figure 7 shows how the lateral deflection across the central section of the panel varied throughout the test. It will be noted that the deformations are located in the upper half of the panel adjacent to the patch load.

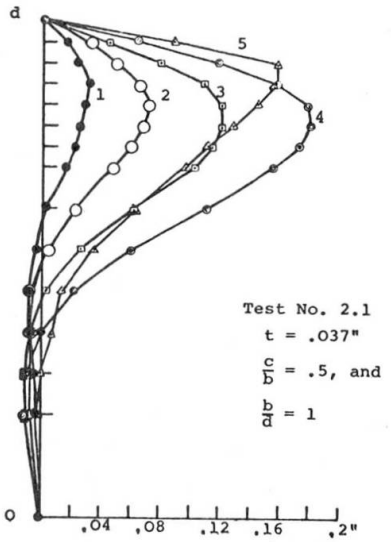


1. P = .485 $P_u$
2. P = .672 $P_u$
3. P = .935 $P_u$
4. P = .999 $P_u$
5. After load removal

Fig. 7. Variation of lateral deflection of web at the mid section with increasing values of the patch load P.

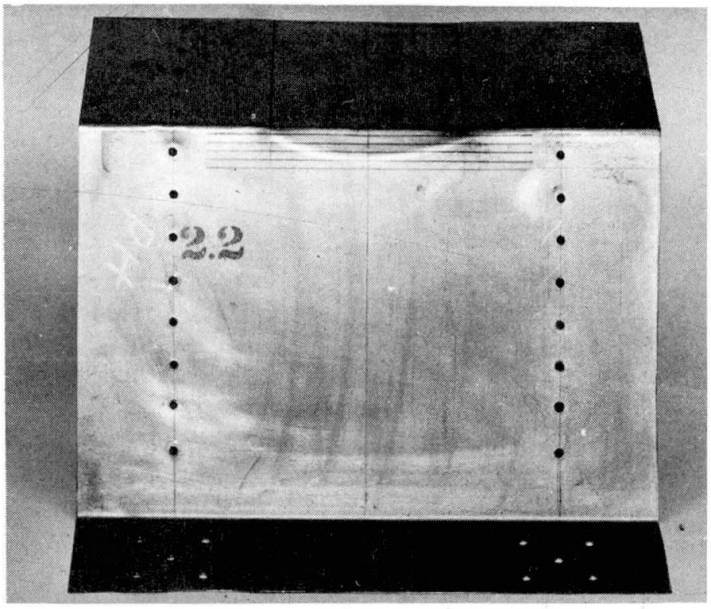


Fig. 8. Failure of a Test Panel showing yield curve.

A most significant result is the failure mechanism, in all of the tests failure occurred by the formation of a local yield curve, as shown in figure 8. This yield curve corresponds closely to a segment of a circle, and has a width equal to that of the patch load. It was also noted that the depth of the curve is proportional to the width of the load as can be seen in figure 9. The grid lines in figure 9 are of equal spacing and the variation in the depth of the curve with the c/b ratio is clearly seen. It was also observed that the shape of the yield curve did not vary with d/t values.

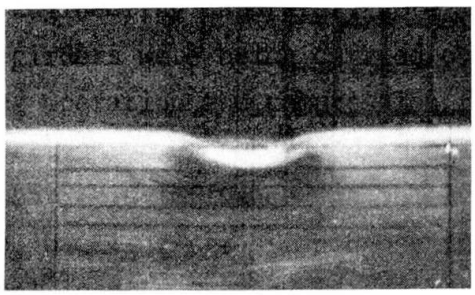

c/b = 0.1 (c = 1.2")

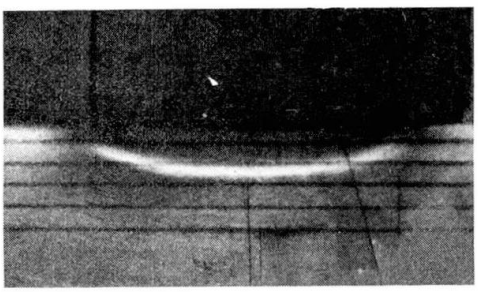

c/b = 0.3 (c = 3.6")

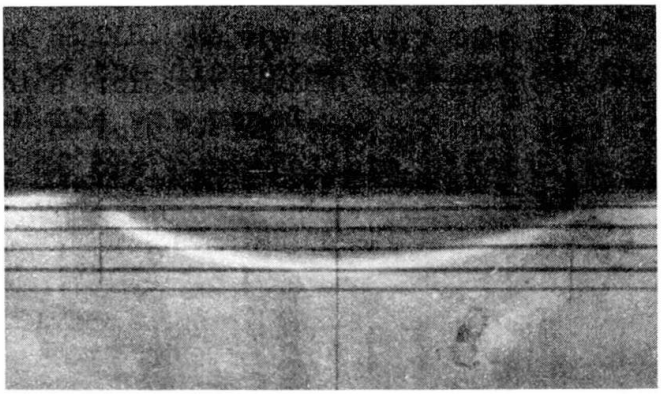

c/b = 0.5 (c = 6.0")

Fig. 9. Yield Curve Shape and Location on Test Panel (b = d)

It can be seen, from table 1, that the ratio $P_u/P_{cr}$ decreases with decreasing values of the d/t ratio and increases with increasing values of the c/b ratio. Figure 10 shows how for the specific case of a panel having a depth to thickness ratio of 200:1, the ratio $P_u/P_{cr}$ varies with the width of the patch load. In figure 11 the $P_u/P_{cr}$ values for the specific cases of c/b = 0.2 and 0.5 and $\alpha$ = 1.0, are plotted against d/t values. From figures 10 and 11 the relationship between $P_u/P_{cr}$, c/b and d/t given in equation 2 has been obtained.

$$\frac{P_u}{P_{cr}} = \left(4.5 + 6.4\left(\frac{c}{b}\right)\right) \frac{d}{t} \times 10^{-3} \qquad (2)$$

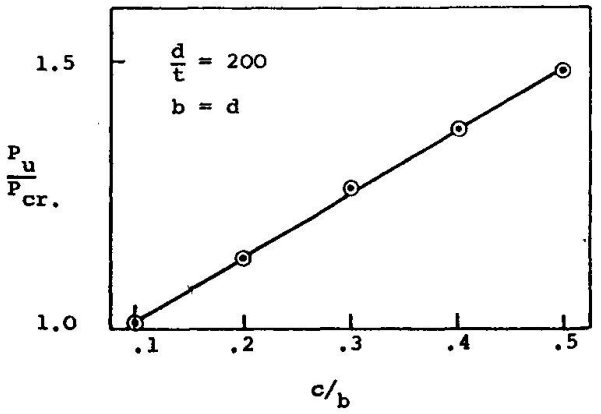


Fig. 10. Variation of the load ratio $P_u/P_{cr}$ with the load parameter ($\beta$).

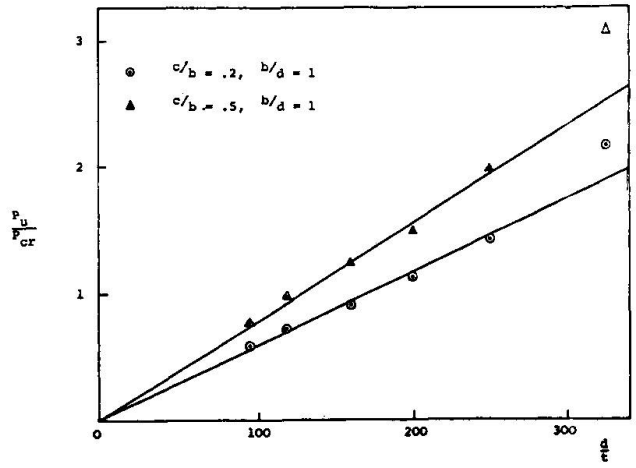


Fig. 11. Variation of the load ratio $P_u/P_{cr}$ with the slenderness ratio (d/t).

Substituting the value of c/b = 1.0 and d/t = 288 into equation 2, it reduces to $P_u/P_{cr}$ = 3.14 which compares closely to the relationship $P_u/P_{cr}$ = 3.0 which Bossert and Ostapenko (11) derived from their tests on panels having a d/t ratio of 288.

The ratios $P_u/P_{cr}$ were found to be smaller for the smaller aspect ratio when $\beta$ is kept constant and equal to 0.2, see table 1. This result contradicts with a conclusion by Bossert and Ostapenko (11) that the post buckling strength varies inversely with the square root of the aspect ratio $\alpha$, when $\beta$ = 1 and d/t = 288. The authors feel that more tests are needed to study the effect of varying $\alpha$, and also to examine the influence of flange stiffness upon the ultimate load characteristics. Currently the authors are examining the effect of the presence of an additional shear or moment, see figures 3 and 4, upon the ultimate load characteristics.

## 5. CONCLUSIONS

The test results have shown that there is a considerable amount of post buckling strength for panels having high slenderness ratios. This post buckling strength also increases with the increase in the loading parameter $\beta$ ($= \frac{c}{b}$). It has been shown that a linear relationship exists between the ratio of the ultimate load ($P_u$) to the buckling load ($P_{cr}$) and the c/b and d/t ratios. Failure of all test panels was defined by the formation of a localised yield curve under the load. The width of this curve was found to be equal to that of the load and its depth proportional to its width.

## ACKNOWLEDGEMENT

This study is based on research work conducted for the British Steel Corporation to whom the authors wish to make grateful acknowledgement.

## NOTATION

| | |
|---|---|
| $b$ | length of panel |
| $c$ | width of patch load |
| $d$ | depth of panel |
| $D$ | flexural rigidity of the plate $\left(= \frac{Et^3}{12(1-\mu^2)}\right)$ |
| $d/t$ | slenderness ratio of panel |
| $E$ | Young's modulus |
| $K$ | non-dimensional buckling coefficient |
| $P$ | applied load |
| $P_{cr}$ | theoretical buckling load |
| $P_u$ | ultimate load |
| $t$ | thickness of plate |
| $\alpha$ | panel aspect ratio, $\frac{b}{d}$ |
| $\beta$ | loading factor, $\frac{c}{b}$ |
| $\mu$ | Poisson's ratio |

## REFERENCES


1. Zommerfield, A.Z., J. Math. Phys. 54 (1906).
2. Timoshenko, S.P., J. Math. Phys. 58, 357 (1910).
3. Girkmann, K., IABSE Final Report (1936).
4. Zetlin, L. Proc. ASCE 81, paper 795 (September, 1955).
5. Wilkesmann, F.W., Stahlbau (October, 1960).
6. White, R.M., and Cottingham, W., J.E.M.Div.Proc. ASCE October (1962).
7. Kloppel, K. and Wagemann, C.H., Stahlbau (July, 1964).
8. Warkenthin, W., Stahlbau (January, 1965).
9. Yoshiki, M., Ando, N., Yamamoto, Y. and Kawai, T., The Society of Naval Architects of Japan, Vol. 12, 1966.
10. Rockey, K.C., and Bagchi, D.K., Int.J.Mech.Sci. Pergamon Press, 1970, Vol. 12, pp. 61 - 76.
11. Bossert, T.W. and Ostapenko, A., Fritz Eng. Lab. Report No. 319.1 (June, 1967).

Leere Seite
Blank page
Page vide